

Jing-wei Li, Zhan-cheng Guo\*, Hui-qing Tang and Jun-cheng Li

# Removal of Impurities from Metallurgical Grade Silicon by Liquation Refining Method

**Abstract:** To develop a new method of refining silicon for use in solar cell materials, liquation refining with Al-Si alloying was proposed for purification of metallurgical grade silicon (MG-Si). The morphologies of impurities, especially for phosphorus and iron, before and after purification were analyzed. By alloying MG-Si with Al, phosphorus in MG-Si formed Al-Si-Ca-P impurity phase and iron formed skeletal-shaped  $\alpha\text{-Al}_8\text{SiFe}_2$  phase into the Al-Si eutectic phase from MG-Si with the presence of Al. It can be concluded that removal mechanism of phosphorus and iron was not only a segregating process, but also a recombining process within certain elements to form specified impurity phases. By centrifugal separation, average separation ratio was 75.73% and average recovery ratio was 82.52% for Al-45%Si system, which is better than traditional separation methods and avoids considerable loss of Al and acid. After refining for four times, mass fractions of phosphorus and boron were reduced to  $0.46 \times 10^{-6}$  and  $0.21 \times 10^{-6}$  respectively. For transition metal impurities, Fe, Ti and Mn, removal fractions of those all were more than 95%.

**Keywords:** metallurgical grade silicon, liquation refining, Al-Si alloy, phosphorus, iron

**PACS® (2010).** 81

**\*Corresponding author: Zhan-cheng Guo:** State Key Laboratory of Advanced Metallurgy, School of Metallurgical and Ecological Engineering, University of Science and Technology Beijing, Beijing 100083, China. E-mail: zcguo@metall.ustb.edu.cn

**Jing-wei Li, Hui-qing Tang, Jun-cheng Li:** State Key Laboratory of Advanced Metallurgy, School of Metallurgical and Ecological Engineering, University of Science and Technology Beijing, Beijing 100083, China

## 1 Introduction

Solar cells are mainly made of multi-crystalline and single crystalline silicon which have advantage of stable quality and high efficiency in conversion from solar to electric energy. Off-spec scrap silicon from the semiconductor industry is used as solar grade silicon (SOG-Si). However, because it is difficult to ensure a steady supply of off-spec

scrap material, a low-cost mass production processes for SOG-Si has been desired [1–3]. Many different approaches [4–10] have been proposed in the field of low-cost silicon feedstock utilization. Among them, a processing route via refining of metallurgical grade silicon (MG-Si) is supposed to offer the best chance of producing SOG-Si at low cost. But its technical problem is to effectively remove boron and phosphorus from MG-Si. These impurities are doping elements for SOG-Si, so their concentrations are required to be controlled below 1ppmw [5]. However, both impurity elements are very difficult to be removed by the directional solidification technique as their segregation coefficients are close to unity.

Liquation refining is a metallurgical method for separating and refining constituents of a metal or an alloy by partial melting when the materials is heated to a temperature where one of the constituents melts and the other remains solid, the liquid constituent can be drained off. So far, a little work has been conducted in alloying MG-Si and utilized the liquation refining to improve the refining process. Some attempts have been made with copper, aluminum or tin et al. as the alloying elements [1, 6, 11, 12]. For Cu-Si system, copper has high affinity for various elements, low activity coefficient and high diffusion coefficient in silicon, which are advantages for remove of most metallic impurities [11]. But Cu-Si alloying could form complex compound resulting difficulty in separating refined Si from the alloy. For Sn-Si system, the segregation coefficient of boron decreased to 0.038 at 1500 K [1], which was much less than 0.8 at the melting point of silicon. Although both boron and phosphorus mass fractions could reduce to  $0.1 \times 10^{-6}$ , the mass fraction of Si in Sn-Si alloy is less than 0.1 at the low temperature. Therefore, the recovery of purified silicon would be insufficient for every alloying treatment. Compared with Cu-Si and Sn-Si alloying, Al-Si alloying is an effective method for purification of MG-Si, because of low segregation coefficients of impurities, especially for boron and phosphorus, between solid silicon and Al-Si melt [1, 12–14], as shown in Fig. 1. But it is difficult to separate purified Si from the Al-Si alloy because of similar density between solid Si and Al. To solve this problem, some external forces, such as electromagnetic force [16] or super gravity [10], were introduced into the silicon refining from Al-Si alloy. Although it could make

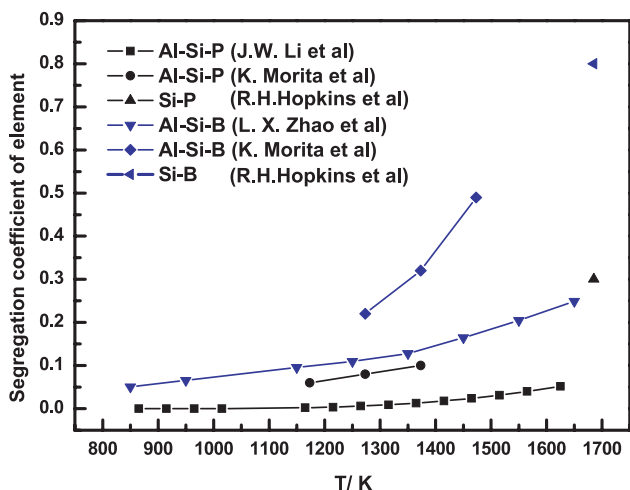


Fig. 1: Segregation coefficients of Boron and phosphorus within Al-Si and Si system [1, 12–14, 16]

the refined silicon agglomeration to some extent and acid leaching is a promising method to selectively collect primary Si from the alloy, it would result in considerable loss of aluminum, and generation of waste acid. Based on the liquation refining method, the refined Si is efficiently separated from the solid-liquid Al-Si alloy avoiding considerable aluminum adhering to the refined silicon grains.

Although some reports [12, 15] have been made that Al-Si alloying could decrease phosphorus and iron contents in the MG-Si, the removal mechanism and transition morphology of impurities have not been elucidated. In this work, the liquation refining method was introduced into the purification of MG-Si with alloying Al. The refined Si grains were separated from Al-Si melt to avoid considerable loss of Al. The morphologies of impurities, especially for phosphorus and iron in silicon grains before and after purification are detected by scanning electron microscope (SEM) and mass fractions of impurities are examined by Inductively Coupled Plasma Optical Emission Spectrometer (ICP-OES). Removal mechanisms of phosphorus and iron were researched in detail based on the structure transformations.

## 2 Experiment

The experimental apparatus is shown in Fig. 2. It consists of a heater and a centrifuge, which could realize the high temperature at the high speed. The centrifugal force was generated by the centrifugal apparatus in the experiment. Fig. 3 shows the flow chart of liquation refining process of MG-Si, which consists of the following steps. First, 22.5 g MG-Si and 27.5 g high purity Al were placed in a dense

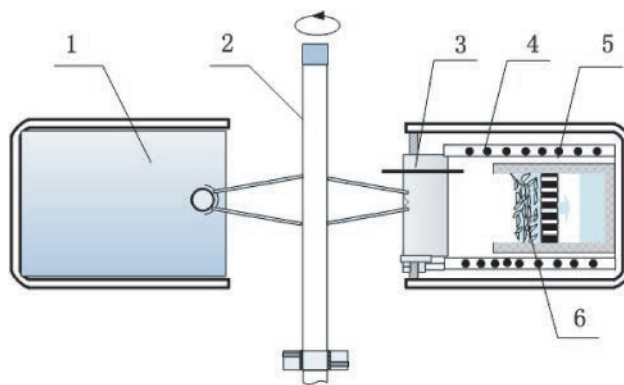


Fig. 2: Schematic sketch of the experimental centrifugal apparatus. 1. Counterweight; 2. Centrifugal axis; 3. Thermocouple; 4. Resistance coil; 5. Alumina filter; 6. Specimen

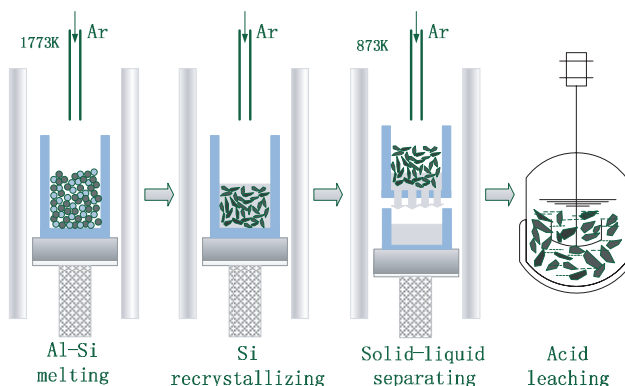


Fig. 3: Flow chart of liquation refining process for the purification of MG-Si

alumina crucible (i.d. = 29 mm) in the muffle furnace. The temperature of the furnace was raised to 1773 K for 2 hours under Ar atmosphere in order to completely fuse. Second, the furnace was cooled down to the room temperature at 3 K/min to make the silicon recrystallized from the Al-Si melt. Third, the solidified Al-Si alloy sample was put into the separation apparatus and the temperature was raised to 873 K for 30 min to reach the solid-liquid state. Then the centrifugal apparatus was started with 1000 rpm for 15 min. In this separation process, the Al-Si hypereutectic melt was ejected from the solid-liquid mixture, and the recrystallized Si was remained in the filter. Then the filter with recrystallized Si was pulled out from the centrifugal apparatus and cooled in an argon protection container to the room temperature. The filter is made of alumina with filter of which slot size was less than 0.5 mm. Last, the recrystallized Si sample was cleaned with aqua regia and HF solution successively to obtain the refined Si. Then, the impurities concentrations in refined Si were examined by

ICP-OES and impurity phases of different stages of liquation refining process were detected by SEM.

### 3 Results and discussion

#### 3.1 Morphology of impurities in the MG-Si

Fig. 4 shows the morphology of impurities in MG-Si, which can be seen from that there are mainly two different impurity phases. EDS analysis indicates that the main impurity phases in MG-Si are Si-Fe matrix (point 1#) and Si-Ca matrix (point 2#) accompanying with a little transition metal elements such as Ti, Ni, Mn, Cr, Cu, V etc. However phosphorus and boron were not detected.

For further investigation of impurity morphologies, especially for phosphorus, the MG-Si was crushed into particles and acid leaching was conducted with aqua regia and HF solution respectively. Fig. 5 shows the mass fraction of phosphorus after different acid leaching. It can be seen that acid leaching has nearly no effect on the removal of phosphorus with different particle sizes. From the literature [17] that acid leaching is effective for the impurities segregated in the grain boundaries, but no effect for the impurities contained in Si matrix. Therefore, it can be concluded that phosphorus was almost completely contained in Si matrix, which results in difficulty to detect and hardly be removed to solar grade level by acid leaching.

#### 3.2 Structure transformation of impurities

In this section, the removal mechanisms of phosphorus and iron were researched in detail by the structure transformation of impurities. As shown in Fig. 1, the segregation coefficient of phosphorus decreased with temperature decrease, which indicated that the smaller the segregation coefficient is, the better the removal efficiency is. Thus, the solidifying process of Al-Si melt plays a key role for the impurities removal. After solidification of Al-Si alloy, the impurities have segregated into the Al-Si eutectics. According to the binary phase diagram of Al-Si system, the eutectic temperature is 850 K. In order to make the eutectics fused and obtain the solid-liquid state, the temperature was fixed at 873 K for Al-45%Si alloy. The purpose of centrifugal process is to separate the semi-solid alloy at this temperature.

Fig. 6(a) shows the macrostructure of Al-45%Si alloy. As can be seen from Fig. 6(a), the solidified macrostruc-

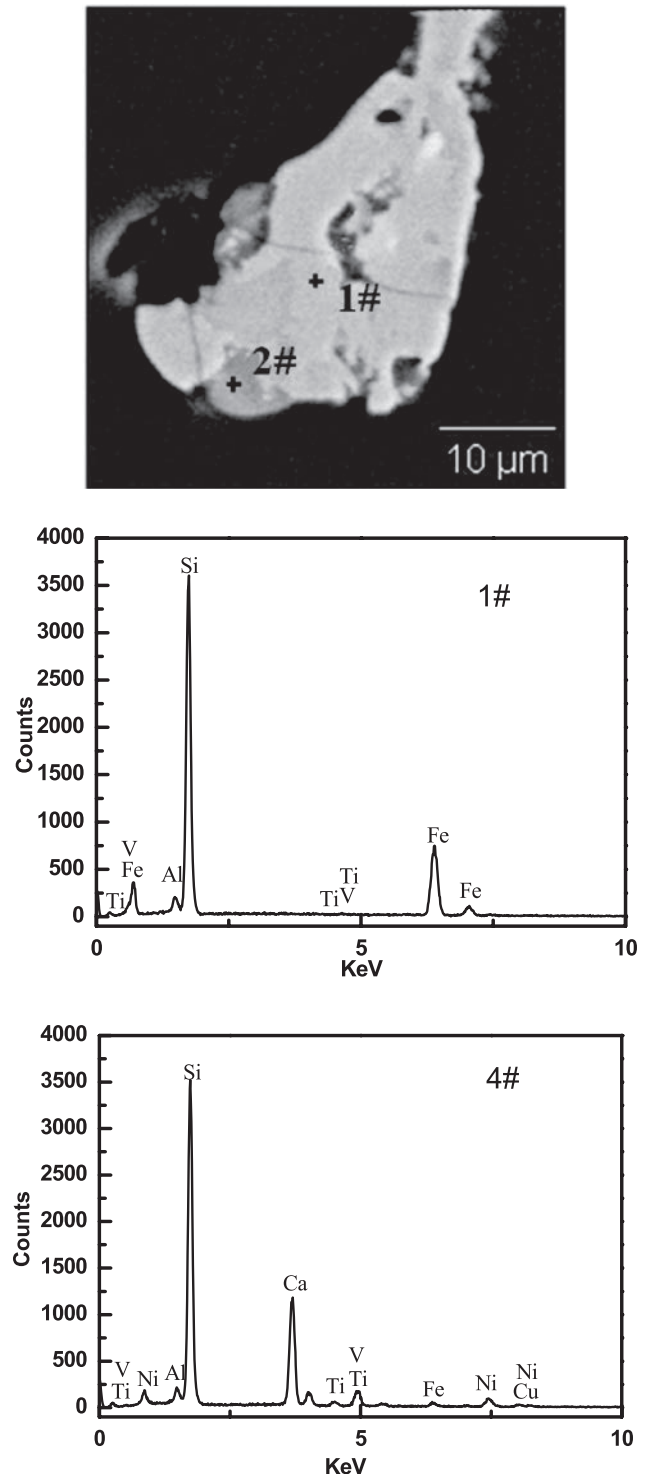


Fig. 4: SEM image of MG-Si corresponding to EDS

ture of Al-45%Si alloy is composed of uniformly distributed needle-like recrystallized Si crystals surrounded by Al-Si eutectics. Because of small density difference between silicon crystals and Al-Si eutectics, the needle-like silicon could not be separated from the Al-Si system

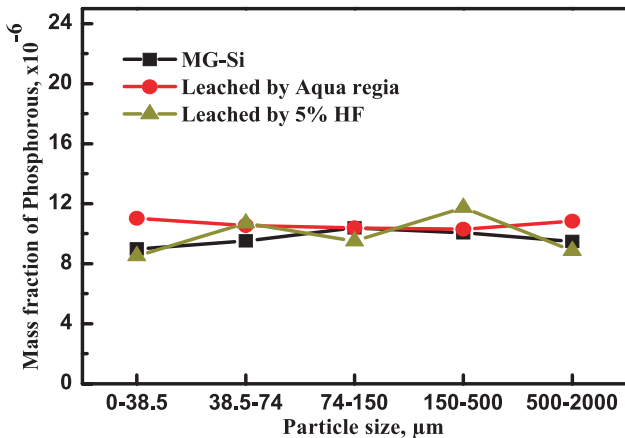


Fig. 5: Comparison of mass fraction of phosphorus in Si after different acid leaching

by gravity sedimentation. For the microstructure analysis of Al-45%Si alloy, some skeletal-shaped impurity phase (point 1) was shown in Fig. 6(b) and EDS analysis of point 1 indicated that it was Al-Si-Fe impurity phase shown in Fig. 6(d). From the literature [18–21], the ternary intermetallic phases for Al-Si-Fe system are of  $\alpha$ -Al<sub>8</sub>SiFe<sub>2</sub>,  $\beta$ -Al<sub>3</sub>FeSi,  $\gamma$ -Al<sub>3</sub>FeSi and  $\delta$ -Al<sub>4</sub>FeSi<sub>2</sub>. Compared with other ternary phases,  $\alpha$ -Al<sub>8</sub>SiFe<sub>2</sub> has the typical skeletal-shaped structure [18]. According to composition of each element, it can be concluded that the Al-Si-Fe impurity phase is  $\alpha$ -Al<sub>8</sub>SiFe<sub>2</sub> intermetallic, combining with characteristic of the skeletal shape. In Fig. 6(c), grey area (point 2) was detected at the boundary of silicon crystals, and EDS result indicates that it is Al-Si-Ca-P impurity phase shown in Fig. 6(e). As mentioned above, phosphorus is contained in Si matrix which results in difficulty to detect and remove. However, by alloying MG-Si with Al, Al-Si-Ca-P impurity phase was formed due to presence of Al and was segregated into Al-Si eutectics which provided an approach for phosphorus removal. Moreover, the morphology of iron changed into  $\alpha$ -Al<sub>8</sub>SiFe<sub>2</sub> phase and was segregated into the Al-Si eutectics.

After the alloying process, centrifugal force was introduced into the separation of recrystallized Si from Al-Si alloy. The morphology of impurity phase in the recrystallized Si was shown in Fig. 7(a). As can be seen from Fig. 7(a), two different impurities phases were detected and both of them located in the Al-Si eutectics. EDS line profile (Fig. 7(b)) indicates that the light grey area (1) was Al-Si-Ca-P impurity phase and the white area (2) was Al-Si-Fe impurity phase. For Al-Si-Ca-P impurity phase, the proportion of each element was relatively fixed, and this result was in accordance with the impurity phase of phosphorus in Al-Si alloy. This result also indicates that some

impurity elements including phosphorus and iron still remain in the recrystallized Si. Fig. 7(c) shows morphology of impurity phase containing phosphorus in the refined Si after acid leaching. As shown in Fig. 7(c), some impurity phase (point 3) was detected in gray area, which was distributed at the grain boundary of Si crystals. EDS result indicates that it was also Al-Si-Ca-P impurity phase.

As mentioned above, the structure transformation of impurities, especially for phosphorus and iron were researched during the different stages of refining process. These results demonstrated that the removal mechanism of phosphorus and iron was not only a segregating process, but also a recombining process to form specified impurity phase. During the alloying MG-Si with Al, phosphorus could form Al-Si-Ca-P impurity phase with the presence of Al and the proportion of each element in the impurity phase was relatively fixed. Iron could change into skeletal-shaped  $\alpha$ -Al<sub>8</sub>SiFe<sub>2</sub> phase. Both of them were segregated into the Al-Si eutectics from MG-Si, which proved that liquation refining was feasible from the perspective of structure transformation of impurities.

### 3.3 Removal fractions of impurities in MG-Si

The impurity contents in the refined-Si together with removal fractions are summarized in Table 1. S1, S2, S3 and S4 represent the times of repeating the entire refining process successively. As can be seen from Table 1, mass fractions of phosphorus and boron decreased with the increase of treatment times. For phosphorus, mass fraction of phosphorus was reduced to  $0.46 \times 10^{-6}$  after four times, removal fraction of that was 97%. For boron, mass fraction of boron was reduced to  $0.21 \times 10^{-6}$  after four times, and the removal fraction of that was 97%. Therefore, mass fractions of phosphorus and boron could be reduced to the solar grade silicon level by multiple treatments. For transition metal impurities, Fe, Ti and Mn, removal fractions of these all exceeded 95%. Al, as the solvent of Al-Si system, remained in the refined Si with low removal fraction. Trumbore's work reported [22] that the solubility of Al in silicon is  $384 \times 10^{-6}$ . Thus, mass fraction of Al was still large after refining.

### 3.4 Effectiveness of the separation of liquid phase

For hypereutectic Al-Si alloy, the total mass of silicon is divided into two parts. One part is recrystallized Si and the



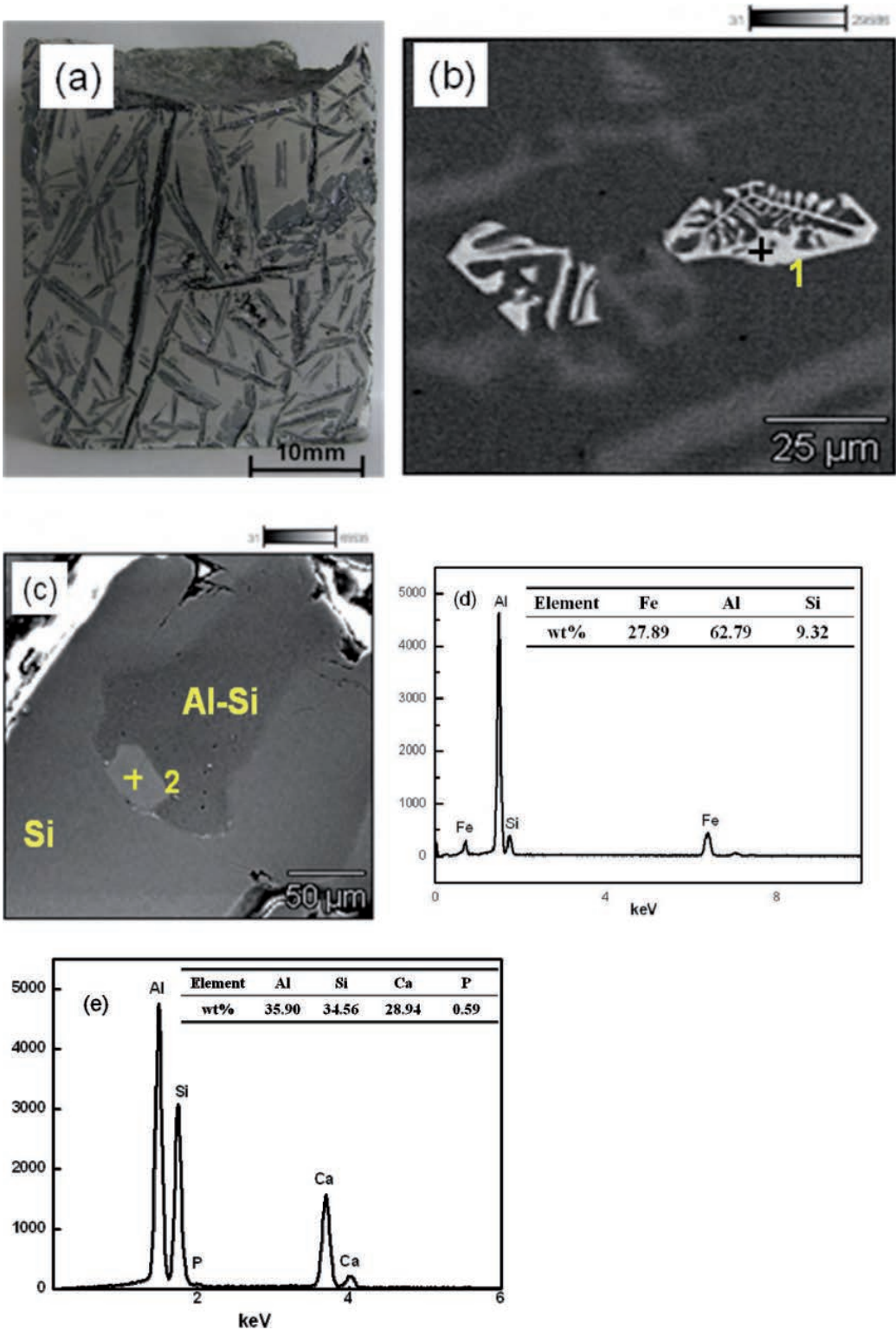


Fig. 6: (a) Macrostructure of Al-45%Si alloy; (b) and (c) SEM images of impurities in Al-45%Si alloy; (d) EDS result of point 1 in (b); (e) EDS result corresponding to point 2 in (c).

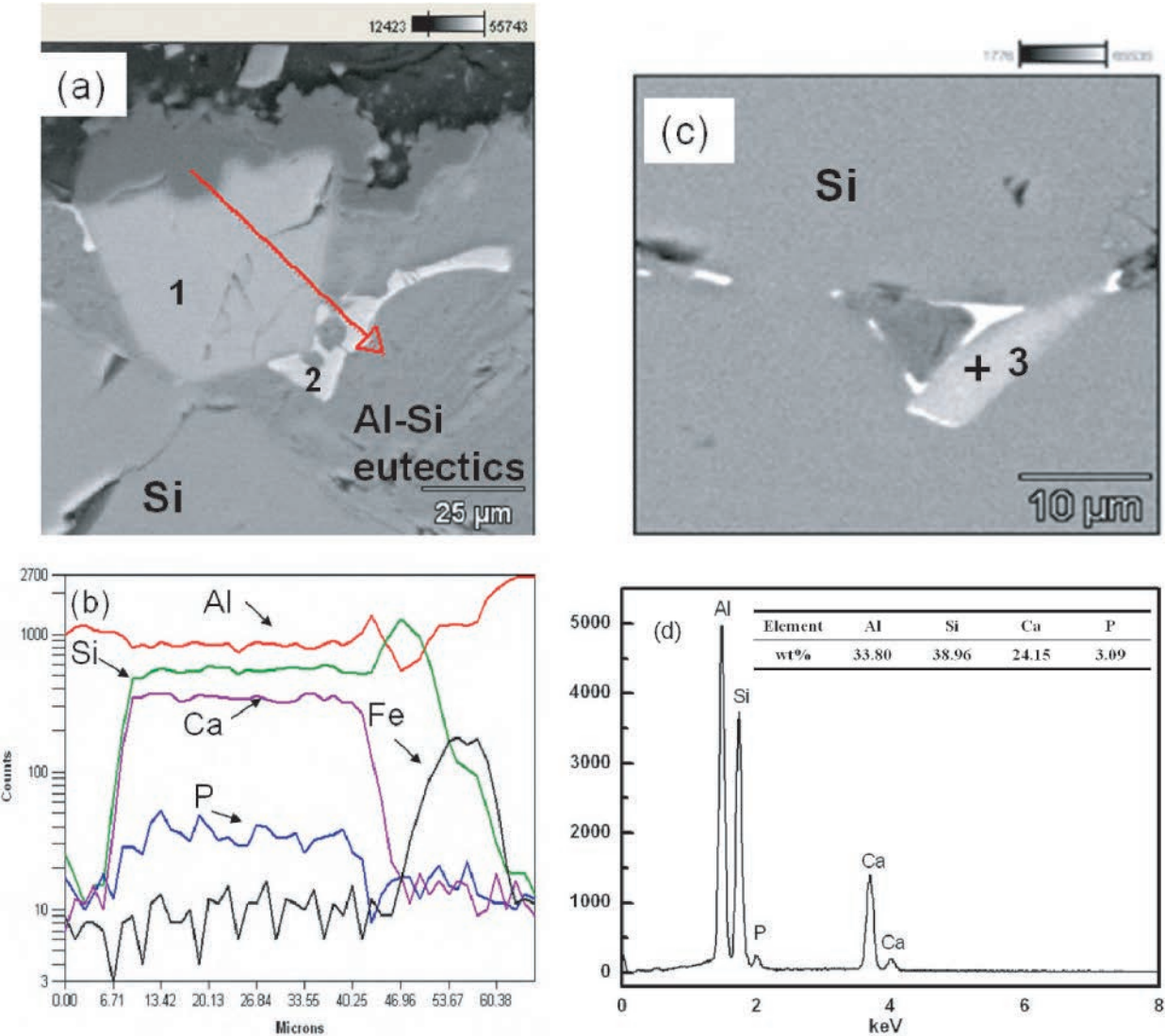


Fig. 7: (a) SEM image of recrystallized Si; (b) EDS line scan of impurity phases in (a); (c) SEM image of refined-Si; (d) EDS result corresponding to point 1 in (c).

Table 1: Impurities content of refined Si and removal fractions after purification

Impurity	Mass fraction ( $\times 10^{-6}$ )					Removal fraction (%)			
	MG-Si	S1	S2	S3	S4	S1	S2	S3	S4
B	8	0.59	0.45	0.24	0.21	93	95	97	97
P	13	3	0.90	0.68	0.46	77	93	95	97
Ti	83	0.11	0.18	0.79	0.24	99	99	99	99
Mn	40	0.68	0.67	1	0.72	98	98	98	98
Fe	1229	35	25	23	20	97	98	98	98
Al	876	359	429	317	386	59	51	64	56

other is located in the eutectics. The refined Si is the recrystallized Si, which does not include that in the eutectics. Besides, some amount of Al-Si eutectics would adhere to the recrystallized Si after the separation. In order to evaluate the effectiveness of the separation of liquid phase, the separation ratio ( $R$ ) was defined as the mass ratio of separated Si to initial Si. The recovery ratio of silicon ( $\eta$ ) was defined as the ratio of actual mass of refined Si to theoretical mass of refined Si. Thus, the separation ratio ( $R$ ) and recovery ratio ( $\eta$ ) were defined as follows:

$$m_{\text{ini}} = m_0 \times a\% \quad (1)$$

$$R(\%) = \frac{m_{\text{sep}}}{m_{\text{ini}}} \times 100 \quad (2)$$

$$m_{\text{id}} = m_0 \times \frac{a\% - b\%}{1 - b\%} \quad (3)$$

$$\eta(\%) = \frac{m_{\text{act}}}{m_{\text{id}}} = \frac{m_{\text{act}} \times (1 - b\%)}{m_0(a\% - b\%)} \times 100 \quad (4)$$

where  $m_0$  is total mass of Al- $a\%$  Si alloy, (g);  $m_{\text{ini}}$  is the mass of initial Si, (g);  $m_{\text{sep}}$  is actual mass of refined Si before acid leaching, (g);  $m_{\text{id}}$  is theoretical mass of refined Si, (g);  $m_{\text{act}}$  is actual mass of refined Si after acid leaching, (g);  $a\%$  is the initial mass percent of Si in Al-Si alloy;  $b\%$  is the Si content of Al-13.6%Si at 873 K (liquidus composition).

The separation ratio ( $R$ ) and recovery ratio ( $\eta$ ) of refined Si were shown in Table 2. As can be seen from Table 2, the average separation ratio was 75.73% for Al-45%Si alloy. According to the Al-Si phase diagram, the theoretical separation ratio is 80.76% at 873 K. The average separation ratio was less than the theoretical ratio, which indicates that the mass of separated Si was reduced during the solid-liquid separation process. Moreover, the average recovery ratio of refined-Si was 82.52% for Al-45%Si system. It can be considered that much silicon grains were leaked from the filter into the Al-Si melt during the separation process. Second, the acid leaching process for recryst-

tallized Si would also cause certain loss of silicon because of the stripping off during acid leaching with aqua regia and erosion effect with HF [23]. Therefore, the actual mass of refined Si would be less than the theoretical value. However, the recycle of remained Al-Si eutectics also needs to be emphasis in order to improve the resource utilization efficiency.

## 4 Conclusion

In this paper, we have proposed an MG-Si purification process with Al-Si melt using liquation refining method, which effectively reduces the concentration of boron and phosphorus. The removal mechanisms of impurities, especially for phosphorus and iron, were researched in detail. During liquation refining process, phosphorus formed Al-Si-Ca-P impurity phase and iron formed skeletal shape  $\alpha\text{-Al}_8\text{SiFe}_2$  phase into the Al-Si eutectic phase from MG-Si with the presence of Al. It can be concluded that removal mechanism of phosphorus and iron was not only a segregating process, but also a recombining process within certain elements to form specified impurity phases. By centrifugal separation, the average separation ratio was 75.73% and the average recovery ratio was 82.52% for Al-45%Si system, which is better than traditional separation methods and avoids considerable loss of Al and acid. After refining for four times, mass fractions of phosphorus and boron were reduced to  $0.46 \times 10^{-6}$  and  $0.21 \times 10^{-6}$  respectively. For transition metal impurities, Fe, Ti and Mn, removal fractions of those all were more than 95%.

**Acknowledgements:** This work was supported by the National Natural Science Foundation of China (51174187), the National Key Technology Research and Development Program of the Ministry of Science and Technology of China (2011BAE03B01).

Received: October 23, 2012. Accepted: February 15, 2013.

**Table 2:** Separation ratio and recovery ratio of refined Si for Al-45%Si alloy

Times	$m_0$ (g)	$m_{\text{ini}}$ (g)	$m_{\text{id}}$ (g)	$m_{\text{sep}}$ (g)	$m_{\text{act}}$ (g)	$R$ (%)	$\eta$ (%)
1	22.1888	9.9850	8.0640	7.5556	6.6489	75.67	82.45
2	13.3489	6.0070	4.8513	4.5958	4.0443	76.51	83.37
3	10.7896	4.8553	3.9212	3.6424	3.2053	75.02	81.74

## References

- [1] L. X. Zhao, Z. Wang, Z. C. Guo and C. Y. Li, Low-temperature purification process of metallurgical silicon, *T. Nonferr Metal Soc.*, 21 (2011), 1185–1192.
- [2] P. Sergio, Towards solar grade silicon: challenges and benefits for low cost photovoltaics, *Sol. Energy Mater. Sol. Cells.*, 94 (2010), 1528–1533.
- [3] B. N. Mukashev, K. A. Abdullin, M. F. Tamendarov, T. S. Turmagambetov, B. A. Beketov, A. M. R. Page and D. M. Kline, A metallurgical route to produce upgraded silicon and monosilane, *Sol. Energy Mater. Sol. Cells.*, 93 (2009), 1785–1791.
- [4] D. Sarti and R. Einhaus, Silicon feedstock for the multi-crystalline photovoltaic industry, *Sol. Energy Mater. Sol. Cells.*, 72 (2002), 27–40.
- [5] A. F. Braga, S. P. Moreira, P. R. Zampieri, J. M. G. Bacchin and P. R. Mei, New processes for the production of solar-grade polycrystalline silicon: a review, *Sol. Energy Mater. Solar Cells.*, 92 (2008), 418–424.
- [6] K. Morita and T. Yoshikawa, Thermodynamic evaluation of new metallurgical refining processes for SOG-silicon production, *T. Nonferr Metal Soc.*, 21 (2011), 685–690.
- [7] T. Miki, K. Morita and N. Sano, Thermodynamics of phosphorus in molten silicon, *Metall. Trans. B*, 27 (1996), 937–941.
- [8] T. Shimpo, T. Yoshikawa and K. Morita, Thermodynamic study of the effect of calcium on removal of phosphorus from silicon by acid leaching treatment. *Metall. Trans. B*, 35 (2004), 277–284.
- [9] T. Yoshikawa, K. Arimura and K. Morita, Boron removal by titanium addition in solidification refining of silicon with Si-Al melt. *Metall. Trans. B*, 36 (2005), 837–842.
- [10] J. W. Li, Z. C. Guo, H. Q. Tang, Z. Wang and S. T. Sun, Si purification by solidification of Al-Si melt with super gravity. *T. Nonferr Metal Soc.*, 22 (2012), 958–963.
- [11] M. Aleksandar, T. A. Mitrasinovic and Utigard, Refining silicon for solar cell application by copper alloying. *Silicon*, 1 (2009), 239–248.
- [12] T. Yoshikawa and K. Morita, Refining of silicon by the solidification of Si-Al melt with electromagnetic force. *ISIJ International*, 45 (2005), 967–971.
- [13] T. Yoshikawa and K. Morita, Refining of silicon during its solidification from a Si-Al melt. *Journal of Crystal Growth*, 311 (2009), 776–779.
- [14] J. W. Li, Z. C. Guo, H. Q. Tang and Y. H. Lin, Thermodynamic evaluation of phosphorus removal within metallurgical grade silicon by fractional melting process, *Proceedings 2012 International Conference on Materials for Renewable Energy and Environment*, Science Technology Publishing, Inc, Beijing, 2012, 15–18.
- [15] X. Gu, X. G. Yu and D. R. Yang, Low-cost solar grade silicon purification process with Al-Si system using a powder metallurgy technique. *Separation and Purification Technology*, 77 (2011), 33–39.
- [16] R. H. Hopkins and A. Rohatgi, Impurity effects in silicon for high efficiency solar cells. *Journal of Crystal Growth*, 75 (1986), 67–79.
- [17] I. C. Santos, A. P. Goncalves, C. Silva Santos, M. Almeida and M. H. Afonso, Purification of metallurgical grade silicon by acid leaching, *Hydrometallurgy*, 23 (1990), 237–246.
- [18] V. Raghavan, Phase Diagram Evaluations Al-Fe-Si (Aluminum-Iron-Silicon), *Journal of Phase Equilibria and Diffusion*, 32 (2011), 140–142.
- [19] P. Skjerpe, Intermetallic phases formed during DC-Casting of an Al-0.25wt pct Fe-0.13wt pct Si alloy, *Metallurgical Transaction A*, 18 (1987), 189–200.
- [20] Y. S. Choi, J. S. Lee, W. T. Kim and H. Y. Ra, Solidification behavior of Al-Si-Fe alloys and phase transformation of metastable intermetallic compound by heat treatment, *Journal of Materials Science*, 34 (1999), 2163–2168.
- [21] L. Eleno, J. Vezely, B. Sundman, M. Cieslar, and J. Lacaze, Assessment of the Al-corner of the ternary Al-Fe-Si system, *Mater. Sci. Forum*, 649 (2010), 523–528.
- [22] F. A. Trumbore, Solid solubilities of impurity elements in germanium and silicon. *Bell System Technical Journal*, 39 (1960), 205–233.
- [23] C. Y. Li, L. X. Zhao, Z. Wang, Z. C. Guo and Y. G. Wang, Removal of representative impurities from metallurgical grade silicon by acid leaching. *The Chinese Journal of Nonferrous Metals*, 8 (2011), 1988–1996 (in Chinese).